SUMO-dependent relocalization of eroded telomeres to nuclear pore complexes controls telomere recombination

Churikov, Dmitri; Charifi, Ferose; Eckert-Boulet, Nadine Valerie; Pinela da Silva, Sonia Cristina; Simon, Marie-Noelle; Lisby, Michael; Géli, Vincent

Published in:
Cell Reports

DOI:
10.1016/j.celrep.2016.04.008

Publication date:
2016

Document version
Publisher's PDF, also known as Version of record

Article

Cell Reports

SUMO-Dependent Relocalization of Eroded Telomeres to Nuclear Pore Complexes Controls Telomere Recombination

Graphical Abstract

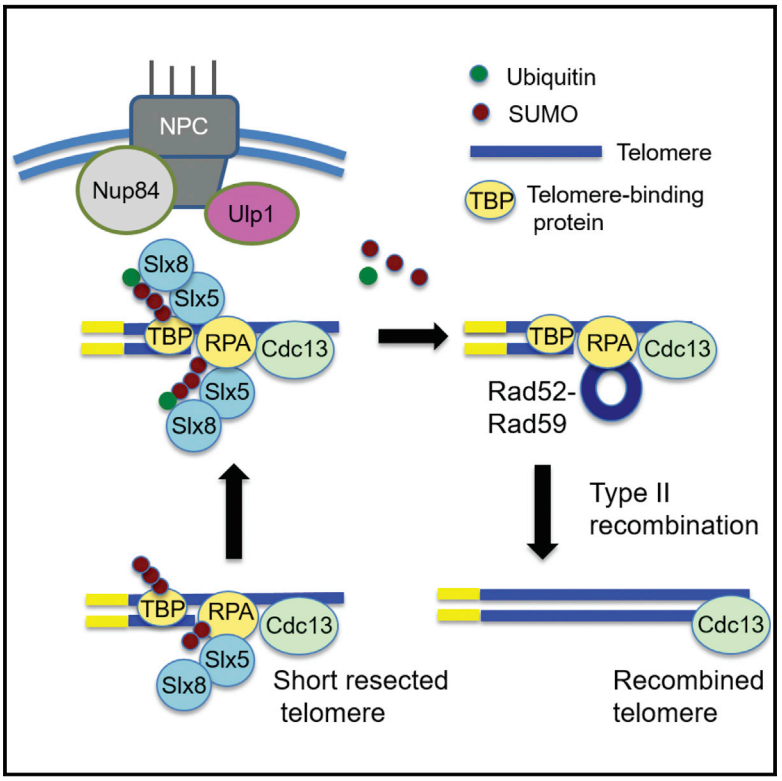

Highlights

- SUMO modification accumulates at eroded telomeres after loss of telomerase
- SUMOlyation promotes recruitment of Slx5-Slx8 STUbL to eroded telomeres
- Rfa1 is SUMOylated during telomere erosion and physically interacts with Slx5
- STUbL-dependent targeting of telomeres to NPCs promotes type II recombination

Authors

Dmitri Churikov, Ferose Charifi, Nadine Eckert-Boulet, Sonia Silva, Marie-Noelle Simon, Michael Lisby, Vincent Géli

Correspondence

marie-noelle.simon@inserm.fr (M.-N.S.), mlisby@bio.ku.dk (M.L.), vincent.geli@inserm.fr (V.G.)

In Brief

Churikov et al. show that eroded telomeres become SUMOylated and recruit Slx5-Slx8 SUMO-targeted ubiquitin ligase. The Slx5-Slx8 complex is essential for telomere relocalization to nuclear pore complexes, a process that promotes the formation of telomerase-independent survivors via type II recombination.

Churikov et al., 2016, Cell Reports *15*, 1242–1253
May 10, 2016
http://dx.doi.org/10.1016/j.celrep.2016.04.008

OPEN ACCESS
CellPress

Cell Reports
Article

SUMO-Dependent Relocalization of Eroded Telomeres to Nuclear Pore Complexes Controls Telomere Recombination

Dmitri Churikov,[1,3] Ferose Charifi,[1,3] Nadine Eckert-Boulet,[2] Sonia Silva,[2] Marie-Noelle Simon,[1,*] Michael Lisby,[2,*] and Vincent Géli[1,*]

[1]Marseille Cancer Research Center (CRCM), U1068 INSERM, UMR7258 CNRS, Aix Marseille University, Institut Paoli-Calmettes (Equipe labellisée Ligue), Marseille 13009, France

[2]Department of Biology, University of Copenhagen, 2200 Copenhagen N, Denmark

[3]Co-first author

*Correspondence: marie-noelle.simon@inserm.fr (M.-N.S.), mlisby@bio.ku.dk (M.L.), vincent.geli@inserm.fr (V.G.)

http://dx.doi.org/10.1016/j.celrep.2016.04.008

SUMMARY

In budding yeast, inactivation of telomerase and ensuing telomere erosion cause relocalization of telomeres to nuclear pore complexes (NPCs). However, neither the mechanism of such relocalization nor its significance are understood. We report that proteins bound to eroded telomeres are recognized by the SUMO (small ubiquitin-like modifier)-targeted ubiquitin ligase (STUbL) Slx5-Slx8 and become increasingly SUMOylated. Recruitment of Slx5-Slx8 to eroded telomeres facilitates telomere relocalization to NPCs and type II telomere recombination, a counterpart of mammalian alternative lengthening of telomeres (ALT). Moreover, artificial tethering of a telomere to a NPC promotes type II telomere recombination but cannot bypass the lack of Slx5-Slx8 in this process. Together, our results indicate that SUMOylation positively contributes to telomere relocalization to the NPC, where poly-SUMOylated proteins that accumulated over time have to be removed. We propose that STUbL-dependent relocalization of telomeres to NPCs constitutes a pathway in which excessively SUMOylated proteins are removed from "congested" intermediates to ensure unconventional recombination.

INTRODUCTION

Telomeres are nucleo-protein structures that protect chromosome ends from degradation, end-to-end fusions, and illegitimate recombination. Telomeres can also recruit telomerase to counteract loss of terminal DNA sequences at the ends of linear eukaryotic chromosomes, which occurs during their replication by conventional DNA polymerases (Pfeiffer and Lingner, 2013). In the budding yeast *S. cerevisiae*, the ends of chromosomes contain a 300-bp array of TG_{1-3} repeats. The essential repressor/activator protein 1 (Rap1) is specifically associated with telomeric duplex DNA repeats, while the extreme ends of telomeres consist of a 12- to 14-nt-long 3′ single-stranded overhang that is bound by Cdc13, a subunit of the CST complex (Cdc13-Stn1-Ten1) (Wellinger and Zakian, 2012). The CST complex plays a major role in telomere end protection, telomere elongation by telomerase, and synthesis of the complementary C strand by DNA polymerase alpha (Churikov et al., 2013).

In addition, telomeres participate in several aspects of the spatial and functional organization of the chromosomes in the nucleus (Taddei and Gasser, 2012). In the budding yeast *S. cerevisiae*, heterochromatic telomeres cluster into three to eight foci at the nuclear periphery, thereby creating a perinuclear compartment enriched in silent information regulator (Sir) proteins. This specialized zone is repressive for transcriptional activity and for canonical homologous recombination (HR) (Schober et al., 2009). Telomere clusters are anchored at the nuclear envelope (NE) through two redundant pathways that involve Sir4 and yKu80, the large subunit of yKu heterodimer (yKu80-yKu70) (Taddei et al., 2004). In S phase, the yKu-specific anchoring pathway requires the telomerase holoenzyme and the integral nuclear membrane protein Mps3 that also contributes to the Sir4-dependent pathway (Bupp et al., 2007; Schober et al., 2009; Oza et al., 2009). In addition, some individual telomeres can be anchored to the nuclear pore complex (NPC). Anchoring to the NPC was shown to be essential for efficient DNA double-strand break (DSB) repair in subtelomeric regions (Therizols et al., 2006).

Telomeres in yeast cells lacking telomerase activity progressively shorten with each cell cycle until they lose capping function and elicit Mec1-dependent growth arrest (Hector et al., 2012). Most of the cells die or remain arrested, but a few cells, called survivors, escape this arrest by rearranging their telomeres via rare recombination events. Two pathways, both requiring Rad52 and Pol32, the nonessential subunit of DNA Polδ, operate to produce telomerase-independent survivors (Teng and Zakian, 1999; Lydeard et al., 2007). Type I survivors that additionally rely on Rad51 carry amplified subtelomeric Y′ elements and have a short terminal TG_{1-3} tracts, while Rad51-independent type II survivors exhibit extended and heterogeneous terminal TG_{1-3} sequences

with minor modifications of subtelomeric repeats (McEachern and Haber, 2006). The type II pathway depends on the MRX (Mre11, Rad50, and Xrs2) complex, Rad59, and the yeast RecQ helicase Sgs1 (Le et al., 1999; Teng et al., 2000; Johnson et al., 2001). Type I survivors arise at a relatively high frequency but grow slowly due to constitutive activation of the DNA damage checkpoint. As a result, type II survivors that arise at a lower frequency but grow robustly take over liquid cultures (Teng and Zakian, 1999). In spite of well-characterized genetic requirements, it proved to be notoriously difficult to analyze recombination events leading to telomere reorganization in survivors due to extremely low frequency of these events (Churikov et al., 2014). We previously characterized the DNA damage response to eroded telomeres in telomerase-negative cells and reported that short telomeres move from their membrane anchor sites to the NPCs (Khadaroo et al., 2009). Similarly, persistent DSBs or replication fork-associated breaks relocalize either to the NPC or to NE protein Mps3 (Nagai et al., 2008; Oza et al., 2009; Kalocsay et al., 2009; Horigome et al., 2014; Chung and Zhao, 2015).

How exactly NPCs contribute to DNA repair is not well understood, but given that SUMO (small ubiquitin [Ub]-like modifier) peptidase Ulp1 localizes at the nuclear basket of NPCs (Zhao et al., 2004) and the similarity of genetic interactions with DNA repair factors displayed by nucleoporins and Ulp1 (Loeillet et al., 2005; Palancade et al., 2007), one part of this contribution may be related to SUMO metabolism. In support of this notion, another member of the SUMO modification pathway, the Slx5-Slx8 heterodimer that constitutes a SUMO-targeted Ub ligase (STUbL) (Xie et al., 2007), was shown to interact with Nup84 complex and to enhance spontaneous gene conversion in an experimental system where a donor sequence was tethered to NPC (Nagai et al., 2008). Very recently, expanded CAG repeats were also shown to transiently relocalize to the NPCs during DNA replication. Impaired relocalization of the expanded CAG repeats in *slx8Δ* and *nup84Δ* mutants correlated with Rad52-dependent expansions and contractions (Su et al., 2015).

Here, we dissect the mechanism by which eroded telomeres are relocalized to the NPCs and the functional consequences of this transaction. We show that telomere erosion at crisis induces an overall increase of telomere-bound protein SUMOylation and that this process is required for telomere relocation to NPC. We further show that Slx5-Slx8 STUbL recognizes SUMOylated eroded telomeres and is essential for telomere relocalization to NPC and type II recombination. We found that replication protein A (RPA), which binds resected telomeres, becomes SUMOylated at the time of crisis and interacts with Slx5-Slx8 STUbL. We propose that relocalization of the eroded telomeres to NPC reflects a pathway involving the Slx5-Slx8-dependent targeting of poly-SUMOylated proteins for either deSUMOylation or proteasomal degradation, a process that facilitates continuous telomere repair attempts.

RESULTS

Telomeres Are SUMOylated upon Their Erosion in the Absence of Telomerase

Previous work established that extended single-stranded DNA (ssDNA) that accumulates in response to DNA damage triggers extensive SUMOylation of a number of HR proteins by the DNA-bound SUMO ligase Siz2 (Cremona et al., 2012; Psakhye and Jentsch, 2012). Therefore, we wondered whether SUMO accumulates at eroded telomeres. To this end, we sporulated heterozygous *EST2/est2Δ* diploids, isolated haploid telomerase-negative *est2Δ* spore clones, and propagated them in liquid cultures via serial dilutions as schematized in Figure 1A (see also Figure S1). As shown for one representative clone, cells went through the telomere erosion-driven crisis and formed survivors (Figure 1B). Typically, *est2Δ* liquid cultures were dominated by type II survivors because of their growth advantage over type I survivors (Figure 1C). We analyzed SUMOylation of telomeres by chromatin immunoprecipitation (ChIP) with an anti-Smt3 (SUMO) antibody followed by dot-blot hybridization with $TG_{1–3}$ probe at different time points of the senescence (Figure 1B). We found that the global level of telomere SUMOylation normalized for the total TG_{1-3} content gradually increased with telomere shortening and then eventually decreased in established survivors with recombined telomeres (Figure 1B). In the input, the intensity of the hybridization signal over time reflected the change of the $TG_{1–3}$ repeats content in agreement with the Southern blot that reveals progressive telomere shortening followed by abrupt telomere elongation via type II recombination (Figure 1C). The increase in SUMOylation appeared to be specific to telomeres, since it was not prominent at rDNA repeats (Figure 1B). Telomere SUMOylation was also detected at the level of individual telomeres using Smt3 ChIP-qPCR, with specific primers in multiple clones (see next section).

SUMOylation of Eroded Telomeres and Efficient Type II Recombination Require Sequestration of the SUMO Protease Ulp1 at NPCs

In budding yeast, the major SUMO-deconjugating enzyme Ulp1 is localized at the nuclear basket of NPCs (Zhao et al., 2004). Such sequestration is believed to limit its uncontrolled access to SUMOylated substrates. Therefore, we took advantage of an Ulp1 mutant, which lacks its N-terminal domain required for NPC localization (Figure 2A) (Li and Hochstrasser, 2003). In spite of decreased level of the ulp1ΔN protein, its mislocalization leads to reduced SUMOylation of specific proteins within the nucleoplasm (Palancade et al., 2007). We reasoned that its delocalization should abolish telomere SUMOylation upon telomere erosion (Figure 2A, right panel). Therefore, we examined global telomere SUMOylation in the *est2Δ ulp1ΔN* mutant by Smt3 ChIP-qPCR at the VI-R, XV-L, and XI-L chromosome ends and at the control loci (Figure 2B). We confirmed by qPCR the accumulation of SUMO at eroded telomeres in the *est2Δ* cells and observed that this increase in the SUMOylation was abolished in the *est2Δ ulp1ΔN* mutant at all chromosome ends analyzed (Figure 2B).

Next, we tested whether SUMOylation of eroded telomeres impacts telomere recombination by evaluating the senescence profiles and the type of survivors formed in multiple *est2Δ* and *est2Δ ulp1ΔN* clones. We found that, on average, *est2Δ ulp1ΔN* clones showed accelerated senescence and a defect of type II recombination (Figures 2C and 2E). Similarly, type II survivor formation was also impaired in *est2Δ* cells lacking the NPC nuclear basket myosin-like proteins 1 and 2 (Mlp1 and Mlp2) (Figures 2D and 2E), which are also required for the proper localization of

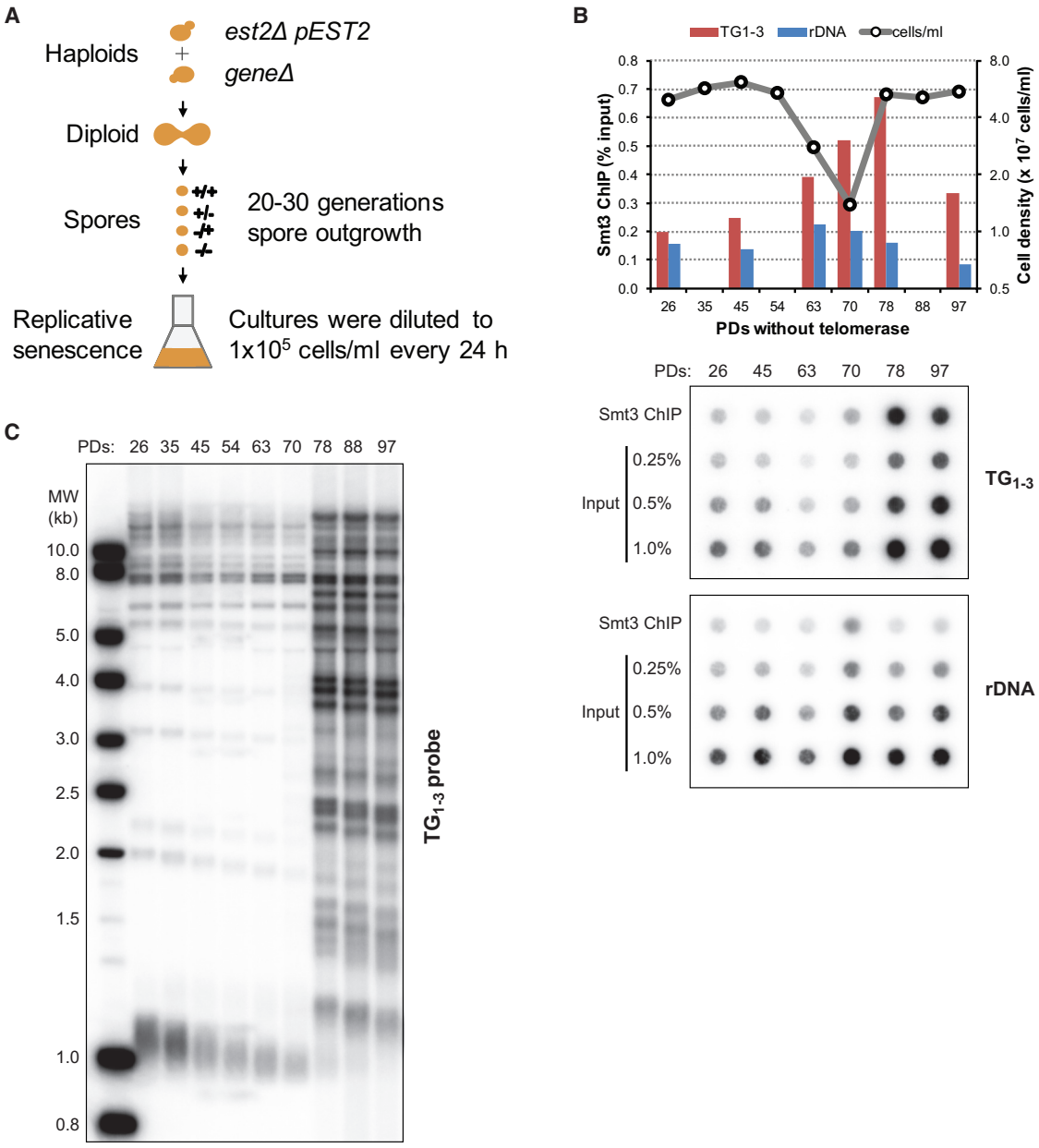

Figure 1. Eroded Telomeres Accumulate SUMO-Modified Proteins

(A) The schematic of the replicative senescence assay. Senescence assays were initiated with telomerase-negative (*est2Δ*) haploid spore clones (at 20–30 PDs) obtained by sporulation of the double-heterozygous diploids (*EST2/est2Δ* and *GeneX/geneXΔ*, where *GeneX* represents any gene of interest). The spore clones were inoculated at 10^5 cells per milliliter into 20 ml of YPD, followed by growth for 24 hr, and the process was repeated until survivors emerged. Cell numbers were estimated by measuring OD_{600}.

(B) The association of SUMO-modified proteins with telomeres in *est2Δ* cells was determined by Smt3 (SUMO) ChIP at the indicated time points (PDs, population doublings starting from *est2Δ* spore). The DNA purified from the chromatin immunoprecipitated with the anti-Smt3 antibodies was dot-blotted on the nylon membrane and hybridized with telomeric $TG_{1–3}$ probe. As a control, the blots were stripped and rehybridized with the rDNA probe. The Smt3 ChIP results were expressed as the percentage of input DNA in ChIPs and plotted on the same graph with the growth curve.

(C) The shortening and recombination of the telomeres in the same replicative senescence experiment (B) was monitored by $TG_{1–3}$-probed Southern blot of *Xho*I-digested genomic DNA. MW, molecular weight.

Ulp1 at NPCs (Zhao et al., 2004). In contrast, *mps3Δ75-150* mutant defective in telomere anchoring to the NE did not exhibit any defect in the formation of type II survivors (Figures S2A and S2B) (Bupp et al., 2007). Altogether, these results are consistent with a positive effect of eroded telomere SUMOylation on type II recombination efficiency.

To further confirm the effect of deSUMOylation of telomere-bound proteins by the spatial delocalization of Ulp1, we adapted

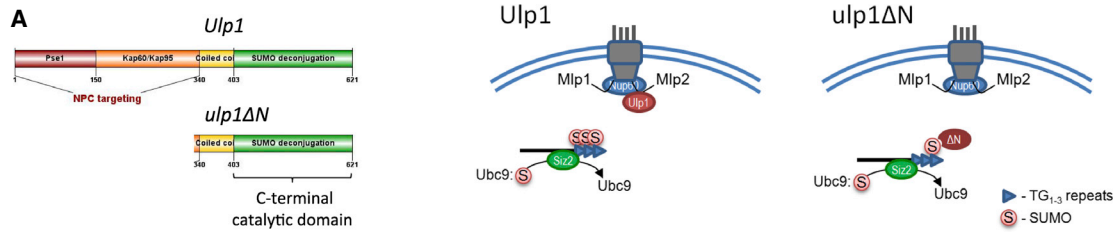

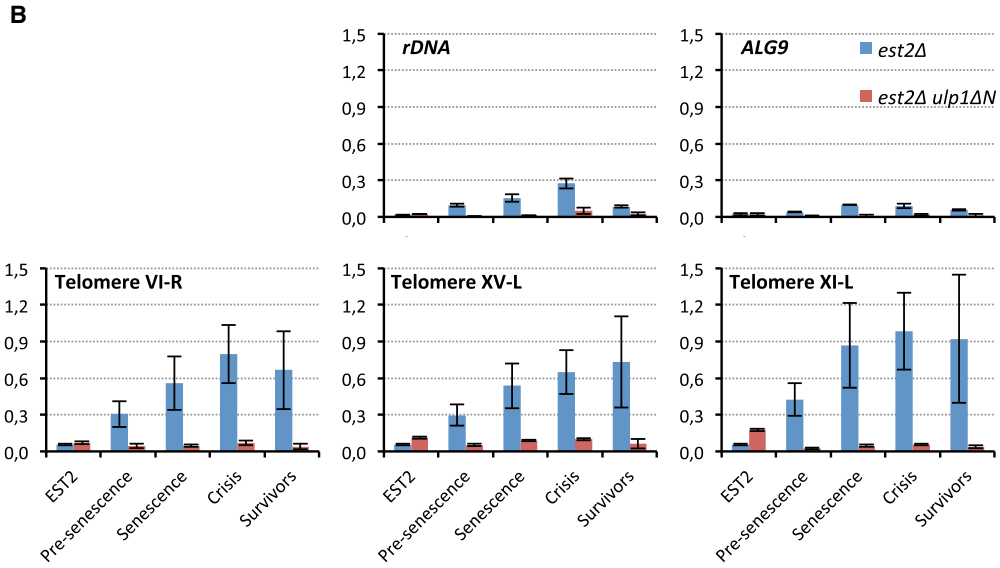

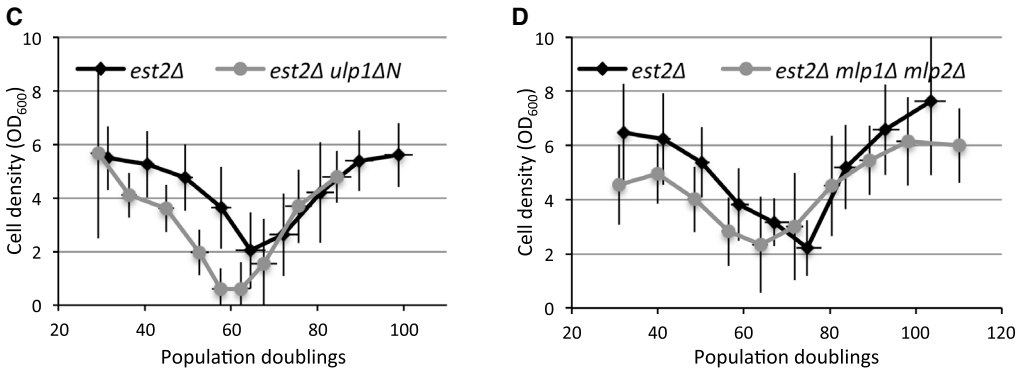

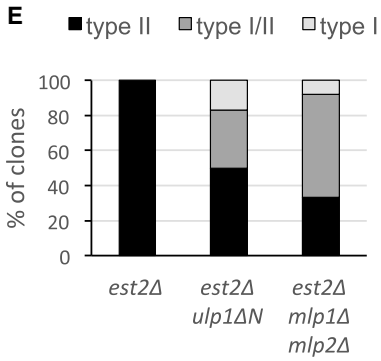

(legend on next page)

a targeting system described by Texari et al. (2013) allowing the tethering of Ulp1 catalytic domain (Ulp1C) to a single telomere. For this purpose, we inserted eight LexA binding sites (8LexAbs) 1.2 kb away from the telomere VI-R (Figure S3) and ectopically expressed either LexA-Ulp1C fusion or LexA protein alone as a negative control (Figure 3A). To quantify the efficiency of type II recombination at TelVI-R, we scored at the first time of growth improvement the number of discrete bands hybridizing with the TelVI-R probe, each corresponding to one TG_{1-3} tract elongation event in the population of senescing cells (Figure 3B). In spite of the possibility of promiscuous activity of the ectopically expressed LexA-Ulp1C at non-targeted chromosome ends, assessment of the type II recombination events across multiple clones revealed that tethering of the Ulp1C to TelVI-R resulted in the statistically significant 2-fold decrease in the frequency of type II recombination at the TelVI-R, while no significant change was detected at the non-targeted TelXV-L (Figure 3C). We concluded that tethering of the catalytic domain of the SUMO protease to TelVI-R negatively affected the efficiency of type II recombination in *cis* but had little effect on recombination in *trans*. Taken together, our data indicate that untimely access of Ulp1 to telomeres by either artificial tethering (LexA-Ulp1C) or global redistribution (*ulp1ΔN*) inhibits telomere recombination and type II survivor formation.

Siz1- and Siz2-Dependent SUMOylation Promotes Eroded Telomere Relocalization to NPCs and Telomere Type II Recombination

Siz1 and Siz2 are responsible for most of the E3-mediated SUMOylation in yeast. Although each E3 ligase has unique substrates in vivo, SUMOylation of many proteins can be stimulated by either one (Reindle et al., 2006). DNA damage has been shown to trigger SUMOylation of a whole suite of proteins involved in the HR-dependent repair (Cremona et al., 2012; Psakhye and Jentsch, 2012). This SUMOylation wave is dependent on the SUMO E3 ligase Siz2, which is recruited to the DNA damage site via interaction with ssDNA-binding complex RPA (Chung and Zhao, 2015). It is thought that SUMO modifications of multiple proteins act synergistically through a combination of SUMO-SIM (SUMO-interaction motif) interactions to accelerate DNA repair.

Therefore, we further investigated whether these SUMO E3 ligases impact senescence rate and telomere recombination (Figures 4A and 4B). While deletion of *SIZ2* alone only slightly decreased the capacity of telomerase-negative cells to form type II survivors, additional inactivation of Siz1 accelerated the senescence rate and increased the type II recombination defect (Figures 4A and 4B), indicating an apparent redundancy in the action of the two SUMO ligases.

Next, we asked whether SUMOylation plays a role in telomere relocalization to NPCs. For this purpose, we used fluorescence microscopy to examine relocalization of the eroded telomeres to NPCs in telomerase-negative mutants lacking the SUMO E3 ligases Siz1 and Siz2. As previously described, we defined, as eroded telomeres under repair, the subset of short telomeres in which Cdc13-YFP (yellow fluorescent protein) and Rad52-RFP (red fluorescent protein) foci colocalized (Khadaroo et al., 2009). We used a strain expressing the *nup133ΔN* mutation, which causes NPCs to cluster at one side of the nucleus while retaining normal DNA repair and mRNA export functions (Khadaroo et al., 2009), to monitor the position of these foci relative to NPC clusters marked by CFP (cyan fluorescent protein)-Nup49 (Figure 4C). While a large proportion of the Cdc13-YFP/Rad52-RFP foci were found at an NPC cluster at the peak of senescence after loss of telomerase in SUMOylation-proficient cells, relocalization of the eroded telomeres to NPCs was compromised after the deletion of either *SIZ1* or *SIZ2* alone and, to a larger extent, in the absence of both Siz1 and Siz2 (Figure 4D).

Together, these results demonstrated that SUMOylation-defective mutants are impaired in the relocalization of eroded telomeres to NPCs in a manner that inversely correlates with the efficiency of type II telomere recombination.

Recognition of the SUMOylated Eroded Telomeres by Slx5-Slx8 STUbL Is Required for Their Relocalization to NPCs and Type II Recombination

The Slx5-Slx8 complex is a STUbL that physically interacts with the Nup84 subcomplex of the NPC (Nagai et al., 2008) and possesses multiple SIMs (Xie et al., 2007). Thus, it constitutes an attractive candidate to mediate an interaction between the SUMOylated eroded telomeres and the NPC. To investigate whether the Slx5-Slx8 complex recognizes eroded telomeres as they progressively shorten and accumulate SUMO in *est2Δ* cells, we examined Slx8 association with telomeric chromatin by ChIP in a strain with Slx8 tagged with GFP at the genomic locus. In parallel, we performed Smt3 ChIP and monitored the state of the telomeres by Southern blot in the same samples. As shown for two independent clones, we recovered increasing amounts of VI-R and XV-L telomere-specific DNA with Slx8-GFP as telomeres shortened, confirming that Slx8 associates with short telomeres (Figures 5A and 5B; see also Figure S4). Furthermore, the timing of Slx8-GFP association with each specific telomere correlated with their SUMOylation, as assessed by Smt3 ChIP (Figure 5A). Interestingly, reduced SUMOylation

Figure 2. Delocalization of the SUMO Protease Ulp1 from NPCs Prevents Eroded-Telomere SUMOylation and Reduces Type II Recombination Efficiency

(A) Schematic of the domain organization of the full-length Ulp1 and ulp1ΔN proteins (left). Cartoon of the delocalization of ulp1ΔN from NPC showing how it may get access to the telomeres and diminish their SUMOylation (right).

(B) Ulp1 delocalization from NPC prevents accumulation of SUMO at eroded telomeres. The association of SUMO-modified proteins with specific telomeres (VI-R, XV-L, XI-L) and control loci (*rDNA*, *ALG9*) in three independent *est2Δ* and *est2Δ ulp1ΔN* clones was determined by ChIP with anti-Smt3 antibody and subsequent qPCR. Data are represented as means ± SEM. Since the time leading up to crisis differs between the strains with different genotypes, the period preceding crisis was divided into two equal parts, "pre-senescence" and "senescence." The crisis itself was defined by the longest PD time (growth nadir).

(C and D) Mean replicative senescence profiles of (C) the *est2Δ* (n = 44) and *est2Δ ulp1ΔN* (n = 20) and (D) the *est2Δ* (n = 5) and *est2Δ mlp1Δ mlp2Δ* (n = 12) clones propagated in liquid cultures. Error bars represent SD.

(E) Relative frequencies of the telomerase-independent survivor types, I and II, for these clones determined by Southern blot analysis.

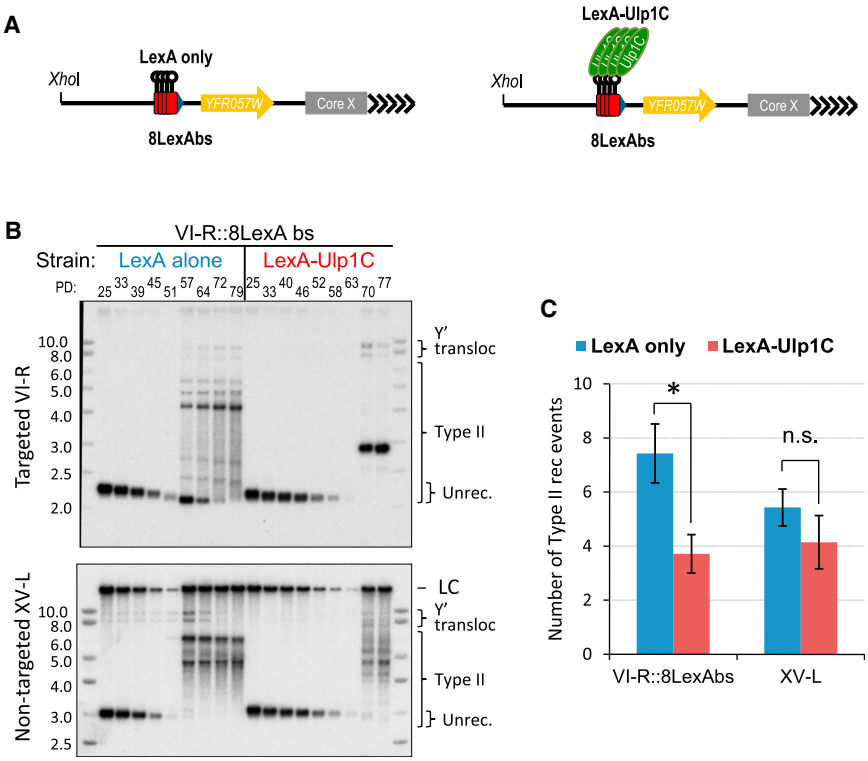

Figure 3. Tethering Ulp1C to TelVI-R Reduces Type II Recombination Efficiency in *Cis*

(A) Schematic of the chromosome VI-R end showing targeting of either LexA or LexA-Ulp1C fusion protein to the 8LexAbs located ~1.2 kb away from the TG_{1-3} repeats.

(B) Representative single-telomere Southern blots hybridized with either VI-R or XV-L probes, which show the timing and the frequency of recombination events at each telomere during outgrowth in the absence of telomerase. Of note, the intensity of any band detected with the VI-R probe in the survivors reflects relative abundance of the survivor clone that arose from a given recombination event but has no relevance to the efficiency of recombination. transloc, translocation; Unrec., unrecombined.

(C) Quantitation of the effect of Ulp1C targeting to telomere VI-R on the frequency of recombination events in *cis* (VI-R) and in *trans* (XV-L). The mean number of type II recombination events (see Results) for each telomere in each strain was plotted. The error bars represent SEM. Seven independent clones of each strain were analyzed. The significance levels (*p = 0.05) are from the unpaired two-tailed t tests. n.s., not significant.

and STUbL binding to telomere XV-L correlated with its delayed and inefficient recombination (compare with telomeres VI-R and XV-L in Figures 5A and 5B).

Next, we deleted *SLX8* and examined eroded-telomere localization relative to NPC in telomerase-negative cells as described earlier. In parallel, the checkpoint-deficient *rad9Δ rad24Δ* mutant was analyzed in the same way. *SLX8* deletion resulted in a drastic reduction of the fraction of Rad52- and Cdc13-containing foci that colocalized with the NPC clusters, while relocalization of eroded telomeres was partially affected in the *rad9Δ rad24Δ* mutant (Figure 5C). Consistent with previous reports, we found that disruption of the Slx5-Slx8 complex led to the production of mainly type I survivors (Figure 5D) (Azam et al., 2006), while inactivation of the DNA damage checkpoint partially affected type II recombination (Figure 5D) (Grandin and Charbonneau, 2007). These results showed that eroded-telomere localization to NPC is greatly dependent on the Slx5-Slx8 complex and that its disruption causes severe type II recombination defect.

RPA Is SUMOylated during Senescence and Physically Interacts with Slx5-Slx8

In response to DNA damage, RPA is SUMOylated on all three subunits, mainly by Siz2 (Cremona et al., 2012; Psakhye and Jentsch, 2012). To verify that Rfa1 is also SUMOylated in response to telomere erosion in *est2Δ* cells, we ectopically expressed His-Smt3 and performed denaturing nickel-nitriloacetic acid (Ni-NTA) pull-down to isolate His-Smt3 conjugates. The presence of Rfa1 in the pull-downs was subsequently analyzed by immunoblotting with anti-RPA antibodies. Indeed, we detected mono- and di-SUMO-Rfa1 in *est2Δ* cells approaching telomere erosion-driven crisis (Figure 6A). Although the pattern of SUMOylated species of Rfa1 in *est2Δ* cells closely resembled that in methyl methanesulfonate (MMS)-treated cells, the fraction of the SUMOylated Rfa1 was notably lower in *est2Δ* compared to MMS-treated cells, probably because of the heterogeneity of the population of senescing cells. Rfa1 SUMOylation returned to the background level when survivors were formed in *est2Δ* culture.

One role that STUbLs plays in DNA repair is to recognize SUMOylated substrates and target them for Ub-dependent degradation, thereby promoting protein turnover and efficient progression through repair steps (Jackson and Durocher, 2013). We reasoned that the targets of Slx5-Slx8 STUbL would become hyper-SUMOylated in the absence of Slx5. Therefore, we analyzed the effect of *SLX5* deletion on the SUMOylation levels of Myc-tagged Rfa1 and also of Rad52, which has been shown to be SUMOylated after DNA damage (Sacher et al., 2006). We found that *SLX5* deletion resulted in a pronounced accumulation of Rfa1-Myc signal in the high=molecular-weight area of the gel (Figure 6B), which is likely caused by excessive, possibly poly-SUMOylation of Rfa1 in the absence of Slx5-Slx8 STUbL activity. Notably, *SLX5* deletion had no measurable effect on the Rad52-myc signal (Figure 6B), although Slx5-Slx8 can ubiquitinate Rad52 in vitro (Xie et al., 2007). We infer from these experiments that Rfa1-SUMO bound to eroded telomeres in *est2Δ* cells may be targeted by Slx5-Slx8.

We next asked whether RPA and Slx5-Slx8 proteins stably interact. We tested the interaction between hemagglutinin (HA)-Slx5 (Tan et al., 2013) and untagged Rfa1 by reciprocal co-immunoprecipitation (co-IP). We detected enrichment of Rfa1 in IPs of HA-Slx5, and, reciprocally, HA-Slx5 was recovered

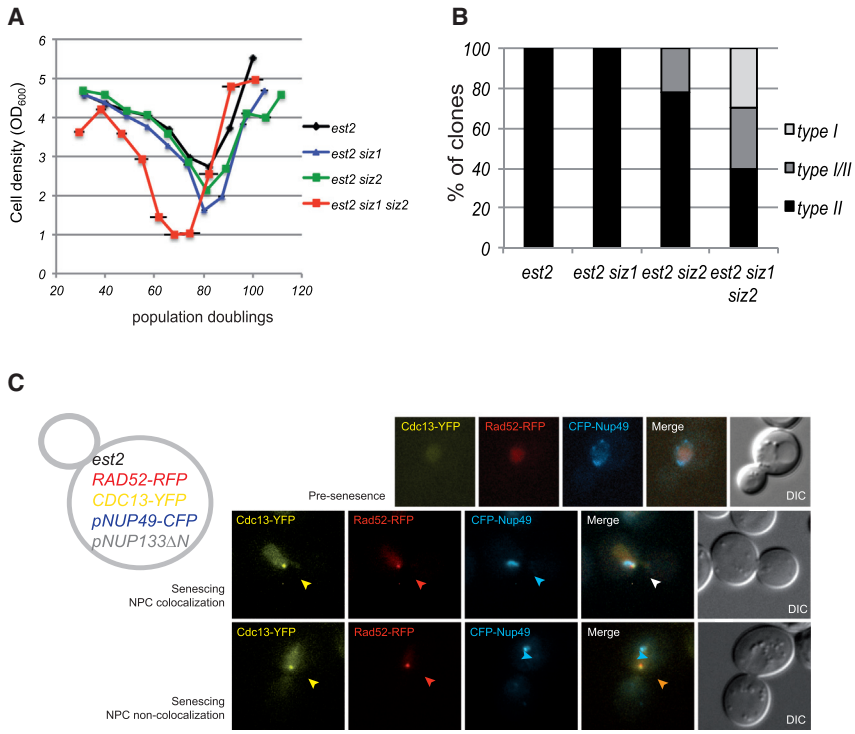

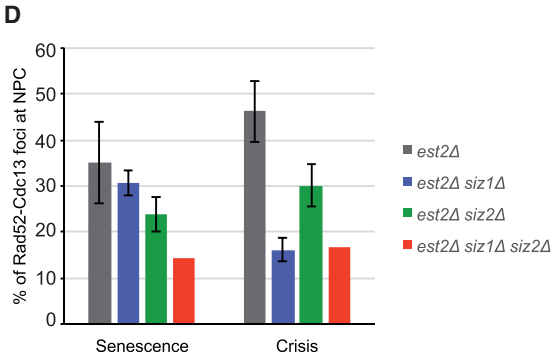

Figure 4. Simultaneous Inactivation of the SUMO E3 Ligases Siz1 and Siz2 Impairs Both Eroded Telomere Relocalization to NPCs and Telomere Type II Recombination

(A) Senescence profiles of the *est2Δ* (n = 3), *est2Δ siz1Δ* (n = 6), *est2Δ siz2Δ* (n = 9), and *est2Δ siz1Δ siz2Δ* (n = 10) clones in liquid cultures. Error bars represent SD.

(B) Relative frequencies of the telomerase-independent survivor types, I and II, for the same clones as in (A) determined by TG_{1-3}-probed Southern blot.

(C) Schematic of the triple-tagged strain used for fluorescence microscopy. Representative images illustrate the presence/absence of eroded telomere colocalization with an NPC cluster. Eroded telomeres were detected as foci containing both Cdc13-YFP and Rad52-RFP, whereas NPC clusters were highlighted by Nup49-CFP in the *nup133ΔN* background, which causes NPCs to cluster at one side of the nucleus.

(D) Quantification of the triple colocalization of Cdc13-YFP, Rad52-RFP, and Nup49-CFP during senescence and at the time of crisis. The data are represented as the means ± SEM for 4, 2, 2, and 1 biological replicates for the *est2Δ*, *est2Δ* siz1Δ, *est2Δ siz2Δ*, and *est2Δ siz1Δ siz2Δ* mutants, respectively.

from anti-RPA precipitates (Figure 6C). Treatment of the extracts with DNase I did not prevent the co-IP of HA-Slx5 and Rfa1 (Figure 6D). Thus it is unlikely that interaction between the two proteins is bridged by DNA.

Artificial NPC Anchoring of TelVI-R Promotes Type II Recombination but Cannot Bypass the Requirement for Slx5-Slx8

We further examined the relationship between NPC localization and type II recombination by artificial tethering of one telomere to the NPC in telomerase-negative cells. Since *est2Δ* cells grown in liquid culture produce predominantly type II survivors, the impact of TelVI-R tethering to the NPC could be monitored only in a mutant strain exhibiting a defect in type II telomere recombination. We chose to use a strain deleted for the SAGA subunit encoded by *ADA2* that exhibits type II telomere recombination defect (Figures S5A and S5B). To tether a single telomere to the NPC, we expressed a LexA-Nup60 fusion protein (Texari et al., 2013) in an *ada2Δ nup60Δ est2Δ* strain carrying 8LexAbs integrated near telomere VI-R (Figure 7A). Such a system was shown to successfully tether *GAL1* to the NPC (Texari et al., 2013). Expression of LexA-Nup60 fully rescued the hydroyurea sensitivity of the *nup60Δ* mutant (Figure S5C).

The state of the TelVI-R was analyzed by Southern blot over the course of senescence and survivor formation as described earlier (Figures 7B and 7C). Analysis of multiple clones indicated that tethering of TelVI-R to the pore resulted in a significant 3-fold increase of the number of type II recombination events in the population of cells as compared to the unmodified TelVI-R control clones (Figure 7C). As an internal control, we probed the unmodified TelXV-L (Figures 7B and 7C) and found similar recombination efficiency in both strains. These data suggest that tethering-eroded telomeres to the NPC provides a molecular environment that improves type II telomere recombination, at least in the context of the *ada2Δ* mutant.

To test whether the type II survivor formation defect observed in the strains deleted for either *SLX5* or *SLX8* is caused solely by impaired localization of eroded telomeres to NPC, we used the same telomere-to-NPC tethering approach to evaluate whether it can also improve type II recombination at TelVI-R in the *slx5Δ* mutant. As described earlier, type II recombination efficiency was evaluated by scoring the number of discrete bands

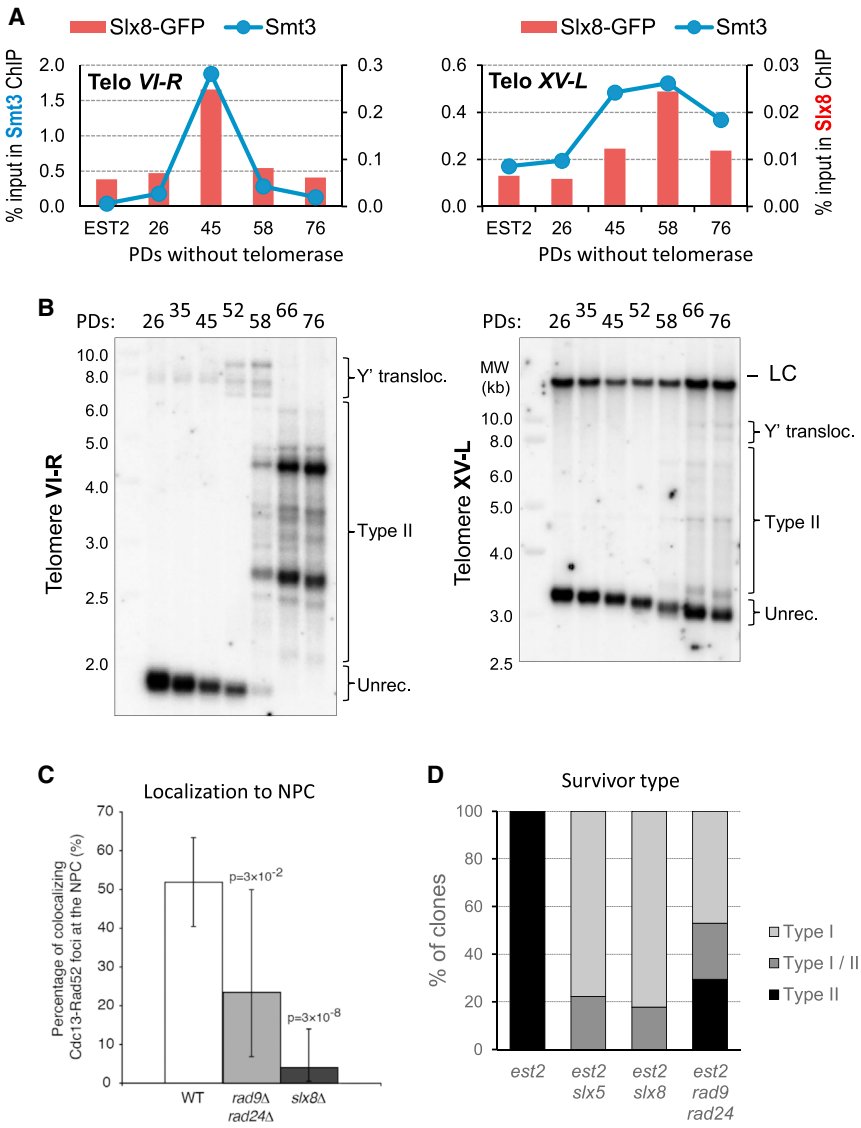

Figure 5. Slx5-Slx8 Complex Binds to SUMOylated Telomeres and Is Required for Both Eroded Telomere Relocalization to NPCs and Type II Recombination

(A) SUMOylated telomeres are recognized by Slx5-Slx8 STUbL. The association of Slx8-GFP- and SUMO-modified proteins with two telomeres was determined in parallel by anti-GFP and anti-Smt3 ChIP-qPCR, respectively, at the indicated time points after telomerase inactivation. The data are shown for one representative *SLX8-GFP est2Δ* clone.

(B) The timing and efficiency of telomere type II recombination is closely correlated with their recognition by Slx5-Slx8 STUbL analyzed by ChIP-qPCR in (A). Southern blot analysis of the same *SLX8-GFP est2Δ* clone as in (A). Note that telomere XV-L, which is poorly SUMOylated, and is weakly bound by STUbL as compared to telomere VI-R, also undergoes delayed and inefficient type II recombination. MW, molecular weight; transloc., translocation; Unrec., unrecombined; LC, loading control.

(C) Inactivation of the Slx5-Slx8 STUbL in *est2Δ* cells severely reduces relocalization of the eroded telomeres to the NPCs. WT, wild-type. p values indicate comparison to the WT (χ^2 test). Error bars indicate exact binomial 96% CIs.

(D) Relative frequencies of the telomerase-independent type I and II survivors in the *est2Δ* (n = 10), *est2Δ slx5Δ* (n = 5), and *est2Δ slx8Δ* (n = 4) clones and in *est2Δ* (n = 10) and *est2Δ rad9 rad24Δ* (n = 14) determined by Southern blot analysis with TG_{1-3} probe.

hybridizing with the TelVI-R and TelXV-L probes (Figure 7D). We did not measure any statistically significant improvement of type II recombination efficiency due to tethering of the TelVI-R to NPC as compared to the non-tethered telomere XV-L (Figures 7D and 7E). We concluded that artificial tethering of a telomere to NPC could not bypass the lack of Slx5-Slx8 STUbL activity in telomere type II recombination.

DISCUSSION

We have previously shown that eroded telomeres relocalized to NPCs when recognized as DNA damage in telomerase-negative yeast (Khadaroo et al., 2009). Although this was a tantalizing observation, particularly in light of the findings that persistent DSBs and long tracts of CAG repeats also tend to localize to NPC where their repair is enhanced (Nagai et al., 2008; Su et al., 2015), neither the mechanism of such relocalization nor its functional significance for the fate of eroded telomeres was understood. In this study, we show that SUMOylation of telomere-bound proteins increases as telomeres shorten in the absence of telomerase with a peak during telomere-erosion-driven crisis and is required for proper telomere relocalization to NPCs. We further showed that the Slx5-Slx8 STUbL is recruited to telomeres as they become sumoylated and plays a crucial role in telomere targeting to NPC. Since Slx5-Slx8 interacts with both the Nup84 complex of NPCs (Nagai et al., 2008) and the SUMOylated protein at telomeres, it may indeed tether the two. Finally, we found that formation of type II survivors, which is dependent on a very specific and still poorly understood mode of Rad51-independent HR, appears to benefit from telomere SUMOylation, telomere relocalization to NPCs, and the proper localization of Ulp1 at the NPCs.

Interestingly, the lack of Slx5-Slx8 STUbL causes much greater defect in type II recombination than when telomere SUMOylation is reduced by disrupting Siz1 and/or Siz2. Since in both cases the relocalization of telomeres to NPCs is reduced, this difference suggests an additional role of STUbL in telomere type II recombination. As type II recombination is particularly dependent on relocalization to NPCs in SUMOylation-proficient cells, the essential role of Slx5-Slx8 STUbL activity in telomere

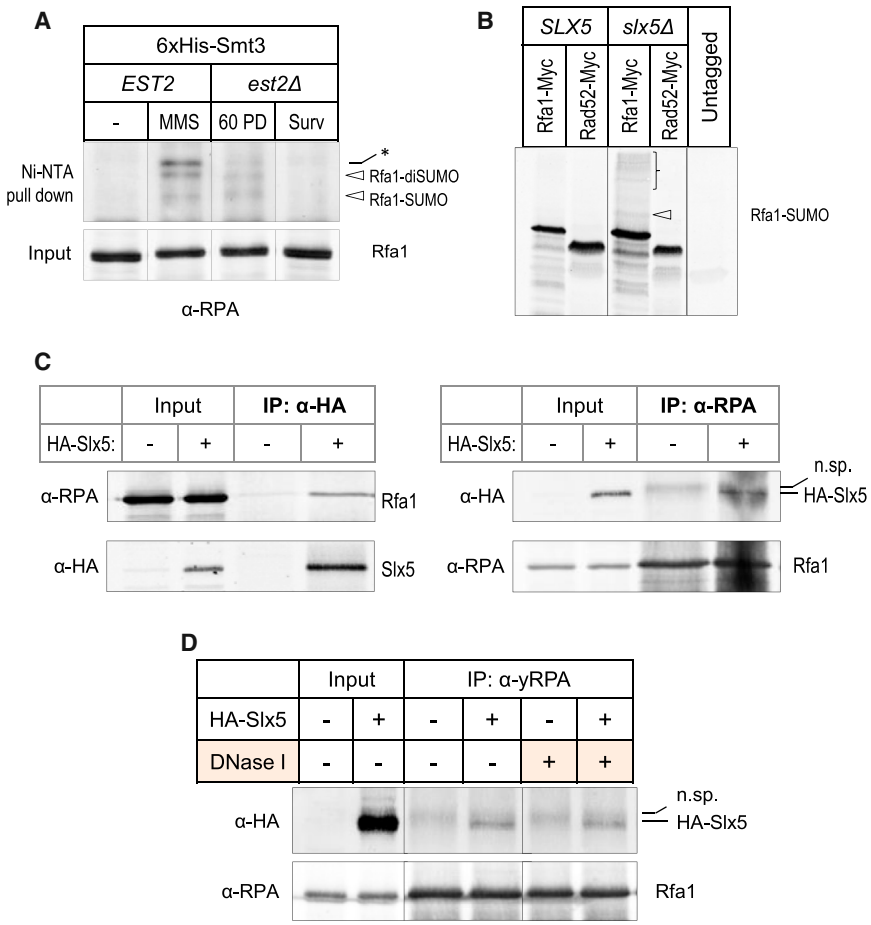

Figure 6. RPA Is SUMOylated during Senescence and Physically Interacts with Slx5-Slx8

(A) Rfa1 is SUMOylated in the *est2Δ* cells approaching crisis. Denaturing Ni-NTA pull-downs were performed to isolate 6xHis-Smt3 conjugates from the telomerase-positive (treated or not with 0.2% MMS) and telomerase-negative cells (either approaching crisis or after formation of the survivors). The presence of SUMOylated Rfa1 in the pull-downs was detected by anti-RPA immunoblotting. The band migrating above the diSUMOylated Rfa1, marked with an asterisk, likely results from a combination of SUMO with another modification (e.g., phosphorylation).

(B) Anti-Myc immunoblot showing that high molecular weight (HMW) Rfa1 species, likely containing poly-SUMOylated Rfa1, accumulate in the cells lacking Slx5. In contrast, lack of Slx5 does not affect the migration of Rad52.

(C) Reciprocal co-IP of the HA-Slx5 and Rfa1 proteins. The presence of Rfa1 in the anti-HA (3F10) immunoprecipitate was determined by anti-RPA immunoblotting, and reciprocally, the presence of HA-Slx5 in the anti-RPA immunoprecipitate was determined by anti-HA (12CA5) immunoblotting. Co-IP was not observed when HA-Slx5 was not expressed. The faint Rfa1 band detected in the anti-HA immunoprecipitate is a common background due to RPA sticking to the beads. The fuzzy band migrating just above the HA-Slx5 in the anti-RPA immunoprecipitate is due to cross-reactivity of the anti-HA antibody with unknown protein precipitating with anti-RPA serum. n.sp., non-specific.

(D) To verify DNA-independent interaction between HA-Slx5 and Rfa1, the extracts were treated with DNase I (100 μg/ml) for 30 min on ice prior to IP. The presence of HA-Slx5 in the anti-RPA immunoprecipitates was determined by anti-HA (12CA5) immunoblotting. n.sp., non-specific.

type II recombination could be related to promoting turnover of certain proteins that become hyper-SUMOylated when telomere recombination is blocked. Since Slx5-Slx8 has multiple SIMs and preferentially interacts with poly-SUMO chains (Mullen and Brill, 2008), its recruitment to telomeres suggests that they accumulate poly-SUMOylated protein(s). Hyper-SUMOylation of several DNA repair factors is known to occur when the downstream repair reactions are inhibited (Sarangi and Zhao, 2015). Accordingly, we found that RPA, which is recruited to resected telomeres (Khadaroo et al., 2009), becomes SUMOylated during the peak of telomere erosion in the absence of telomerase and is hyper-SUMOylated in the absence of Slx5-Slx8. Similarly, the mammalian STUbL RNF4 is required to prevent RPA hyper-SUMOylation (Galanty et al., 2012). We do not think that RPA is the only hyper-SUMOylated target of Slx5-Slx8 at eroded telomeres, but it might be the primary one. In support of this notion, we found that Slx5-Slx8 physically interacts with unmodified RPA, and thus, ssDNA-bound RPA may serve as a landing pad for the Slx5-Slx8 recruitment to resected telomeres. It is possible that continuous SUMOylation of RPA by Siz2 in response to persistent DNA damage enhances its interaction with Slx5-Slx8, which results in the localized retention of STUbL activity. In addition, the DNA damage checkpoint also affects relocalization of telomeres to NPCs, which may be related to proper DNA end resection (Cremona et al., 2012). These results suggest that large regions of ssDNA covered by hyper-SUMOylated RPA may constitute the initial signal that triggers the relocalization of various unrepairable DNA lesions to NPCs (Géli and Lisby, 2015).

There are two possible ways whereby relocalization to NPCs may promote deSUMOylation of telomere-bound proteins. One way of deSUMOylation at NPCs is via the nuclear-basket-associated Ulp1, while another one is Ub-dependent targeting of the poly-SUMOylated substrates for proteasomal degradation (Geoffroy and Hay, 2009). Remarkably, the NPC nuclear basket is part of a dynamic protein network, which includes proteasomes (Niepel et al., 2013). In addition, the Slx5-Slx8 STUbL physically interacts with multiple regulatory subunits of the 26S proteasome lid, including Rpn3, Rpn5, and Rpn11 (Krogan et al., 2006). Therefore, it is tempting to speculate that the shift of the eroded telomeres to NPCs may actually reflect the process of targeting to proteasomes. The presence of both Ulp1

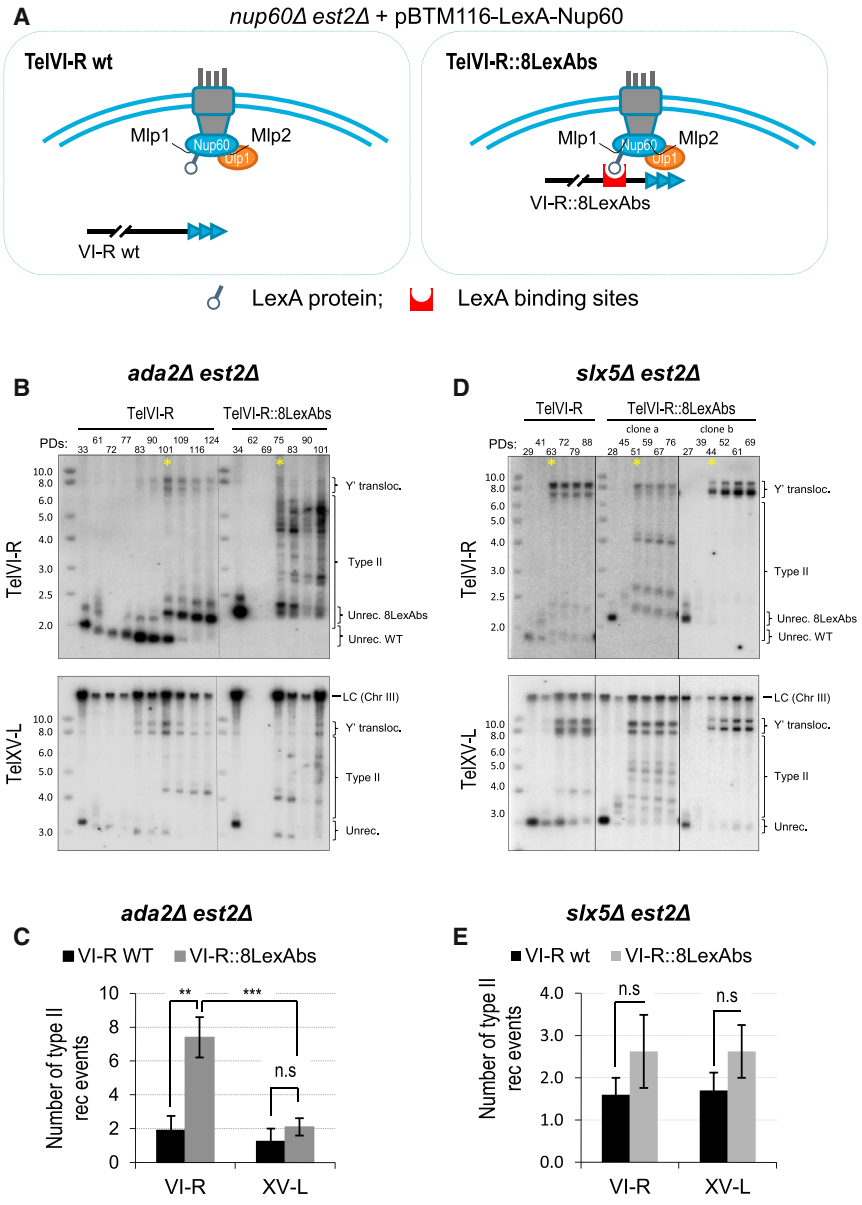

Figure 7. Tethering of the TelVI-R to the NPC Promotes Type II Recombination

(A) Schematic of the two *est2Δ nup60Δ* p*LexA-NUP60* strains bearing either wild-type (wt) or modified VI-R that were used to assay for the effect of TelVI-R tethering to the NPC on the efficiency of type II recombination.

(B) The effect of tethering to NPC on type II recombination was evaluated in *ada2Δ nup60Δ est2Δ* p*LexA-NUP60* cells in *cis* (TelVI-R) and in *trans* (TelXV-L) by Southern blotting using subtelomere-specific probes. The results are shown for two representative clones. DNA was digested with *Xho*I. LC represents a loading control, an internal fragment of chromosome (Chr) III that cross-hybridizes with XV-L probe. Yellow asterisks mark the time point at which the type II recombination events were counted. WT, wild-type; transloc., translocation; Unrec., unrecombined.

(C) Quantification of the effect of TelVI-R tethering to NPC on the frequency of type II recombination (rec) events in *cis* (VI-R) and in *trans* (XV-L) in the *ada2Δ* background. The mean number of type II recombination events was plotted for each telomere in the clones with either unmodified TelVI-R (n = 8) or TelVI-R:8LexAbs (n = 9). The error bars represent SD. The p values were obtained by Fisher's least significant difference (LSD) test. **p < 0.01; ***p < 0.0001; n.s, not significant.

(D) Southern blots as in (C) for the representative *est2Δ nup60Δ slx5Δ* p*LexA-NUP60* strains expressing either unmodified TelVI-R or TelVI-R::8LexAbs.

(E) Quantification of the effect of TelVI-R tethering to NPC on the frequency of type II recombination events in *cis* (VI-R) and in *trans* (XV-L) in the *slx5Δ* background. The data for the clones with either unmodified TelVI-R (n = 10) or TelVI-R:8LexAbs (n = 8) were plotted and analyzed as in (C).

and proteasome at the NPC may facilitate either deSUMOylation or degradation of the SUMOylated proteins at eroded telomeres, thereby giving them an opportunity for another repair attempt.

We propose that telomere repair in telomerase-negative cells is a two-step process (Figure S6). During the first stage, short telomeres with limited levels of single-stranded overhangs would be repaired by subtelomeric sequence translocation and amplification (Churikov et al., 2014). By the time of crisis, the efficiency of this repair is diminished due to shortening of the TG_{1-3} tracts, leading to extensive resection, excessive SUMOylation, and accumulation of telomeres in the form of "congested" recombination intermediates (Géli and Lisby, 2015). These non-repairable telomeres are then targeted to the NPC through a process involving SUMO, RPA, and Slx5-Slx8. Possibly, STUbL and NPC-associated Ulp1 both contribute to the clean-up of polySUMOylated proteins, including RPA, thereby disassembling dead-end intermediates at resected telomeres.

The alternative lengthening of telomeres (ALT), identified in certain human cancer cells, also depends on SUMO-mediated targeting of the telomeres to promyelocytic leukemia (PML) nuclear bodies (Potts and Yu, 2007). Remarkably, the RNF4 STUbL that interacts with RPA (Galanty et al., 2012) and the SMC5/6 complex that is essential for ALT are both recruited to PML bodies (Potts and Yu, 2007). Therefore, the SUMO dependence of the telomere recombination pathways in the absence of telomerase may be conserved between yeast and mammals.

EXPERIMENTAL PROCEDURES

Senescence Assays and Telomere Southern Blot Analysis

Strains, primers, and plasmids used in this study are described in Tables S1, S2, and S3, respectively. Liquid senescence assays were performed starting with the haploid spore products of diploids that were heterozygous for EST2 (*EST2/est2Δ*) and for the gene of interest. To ensure homogeneous telomere length before sporulation, the diploids were propagated for at least 50

population doublings (PDs) in YPD. The entire colonies outgrowing from haploid spores (estimated 25–30 PDs) were inoculated in liquid YPD medium and grown to saturation at 30°C. Every 24 hr, the cell density was measured (optical density at 600 nm; OD_{600}), and a fresh 15 ml of YPD was inoculated with an estimated 10^5 cells per milliliter. Multiple clones of each genotype were propagated in this manner until the emergence of survivors. Replicative senescence curves shown in this study correspond to the average of several senescence experiments using different spores with identical genotype. The senescence assays on solid medium were initiated in the same fashion as described earlier, but the cells were propagated by consecutive restreaking on solid YPD plates followed by outgrowth for 3 days at 30°C. The process was repeated until the appearance of survivors. Terminal restriction fragments (TRFs) containing telomeres were visualized by Southern blotting with a telomeric $TG_{1–3}$ probe. The types of survivors were determined based on their characteristic TRF pattern. For Southern blot analysis, approximately 25 μg of DNA was digested with *Xho*I, resolved in 1% agarose gel, and transferred onto a Hybond-N+ membrane. For bulk telomere analysis, Southern blots were hybridized with radiolabeled telomeric $TG_{1–3}$. For single-telomere analysis, DNA was treated as described earlier, and the blots were probed sequentially with TelVI-R- and TelXV-L-specific probes prepared as described earlier and elsewhere (Churikov et al., 2014). To monitor the efficiency of type II recombination events at TELVI-R and TELXV-L, we scored the number of discrete bands hybridizing with the specific probe at the first time point of type II appearance for each clone analyzed. Each of these bands corresponds to a single type II recombination event, independently of its size (which is stochastic from one recombination event to another) and intensity (that only reflects the relative enrichment of one peculiar survivor in the heterogeneous population of cells).

Integration of the LexAbs into the VI-R Subtelomere for Tethering Experiments

The cassette containing eight tandem LexAbs and floxed *Kluyveromyces lactis URA3* was amplified using the pUG72-8LexA_BS plasmid and the primers VIRpUG72F and VIRpUG72R (Tables S2 and S3). The cassette was then transformed into the W303 pGAL-Cre strain for integration upstream of the *YFR057W* open reading frame (ORF), 1.2 kb away from the $TG_{1–3}$ repeats (Figure S2A). The integrants were selected on SD-Ura dropout plates. Due to strong subtelomeric silencing, small colonies appear 1 week after transformation. The clones were screened for targeted integration by PCR and Southern blotting. Subsequently, Cre-recombinase was induced in galactose medium to remove *KlURA3*. The PCR fragment used to prepare a VI-R-specific probe for Southern blot was generated using the primers given in Table S2. Plasmids pUG72-8LexA_BS (to integrate LexAbs); pLac111-promUlp1-LexA (control plasmid) and pLac111-promUlp1-LexA-Ulp1C (to express the catalytic domain of Ulp1 fused to LexA); and pBTM116-URArev-LexA (control plasmid) and pBTM116-URArev-LexA-Nup60 (to express Nup60 fused to LexA) were kindly provided by Lorane Texari and Françoise Stutz (Texari et al., 2013).

Live-Cell Imaging of Senescing Cells and Fluorescence Microscopy

Live-cell imaging was performed on *est2Δ nup133ΔN* cells expressing Rad52-RFP-, Cdc13-YFP-, and pNup49-CFP-tagged proteins after elimination of the pVL291 vector carrying *EST2* (*URA3*) on 5′-fluoroorotic acid (5′-FOA)-containing plates. Two to four independent Ura- and 5′-fluoroorotic acid resistant ($5'$-FOA^R) colonies were used to inoculate 20-ml liquid cultures in SC-Trp-Leu+Ade medium (100 μg/ml adenine). These cultures were grown in the shaker incubator at 25°C and diluted to OD_{600} = 0.3 every day. At the time of each dilution, an aliquot of cells was examined by fluorescence microscopy. Generation time and PDs were calculated based on OD_{600} measured over consecutive time intervals. Mutant strains (*siz1Δ*, *siz2Δ*, *siz1Δ siz2Δ*, *rad9Δ rad24Δ*, and *slx8Δ*) were obtained by sporulation of respective heterozygous diploids followed by selection of spore clones carrying desired combination of markers.

Fluorescein microscopy was performed as described by Eckert-Boulet et al. (2011). Fluorophores were CFP (clone W7), YFP (clone 10C), and RFP (clone yEmRFP). Fluorophores were visualized on an AxioImager Z1 (Carl Zeiss MicroImaging) equipped with a 100× objective lens (Zeiss PLAN-APO; NA, 1.4), a cooled Orca-ER CCD camera (Hamamatsu), differential interference contrast (DIC), and a Zeiss HXP120C illumination source. Images were acquired and processed using Volocity software (PerkinElmer). Images were pseudocolored according to the approximate emission wavelength of the fluorophores.

Other Methods

Smt3 (SUMO) and GFP ChIP; co-IP; protein pull-down and western blot quantification; and antibodies are described in the Supplemental Information.

SUPPLEMENTAL INFORMATION

Supplemental Information includes Supplemental Experimental Procedures, six figures, and three tables and can be found with this article online at http://dx.doi.org/10.1016/j.celrep.2016.04.008.

AUTHOR CONTRIBUTIONS

D.C. contributed to Figures 1, 2, 3, 5, 6, and 7; F.C. contributed to Figures 1, 2, and 5; M.N. contributed to Figures 2, 4, and 7; N.E.B., S.S., and M.L. contributed to Figures 4 and 5; and D.C., M.N., M.L., and V.G. wrote the manuscript.

ACKNOWLEDGMENTS

We are very grateful to H. Ulrich for the anti-SMT3 antibodies; F. Stutz and L. Texari for their help with the tethering experiments; S. Jentsch, F. Holstege, G. Prelich, Z. Wang, and B. Johnson for strains and plasmids; and F. Jourquin for technical help. V.G. is supported by the Ligue Nationale Contre le Cancer and by L'Institut National Du Cancer (TELOCHROM and PLBIO14-012). M.L. was supported by the Danish Council for Independent Research, the Villum Foundation, and the European Research Council (ERCStG, 242905). S.S. was supported by the Fundação para a Ciência e a Tecnologia.

Received: February 19, 2016
Revised: March 14, 2016
Accepted: March 28, 2016
Published: April 28, 2016

REFERENCES

Azam, M., Lee, J.Y., Abraham, V., Chanoux, R., Schoenly, K.A., and Johnson, F.B. (2006). Evidence that the *S.cerevisiae* Sgs1 protein facilitates recombinational repair of telomeres during senescence. Nucleic Acids Res. *34*, 506–516.

Bupp, J.M., Martin, A.E., Stensrud, E.S., and Jaspersen, S.L. (2007). Telomere anchoring at the nuclear periphery requires the budding yeast Sad1-UNC-84 domain protein Mps3. J. Cell Biol. *179*, 845–854.

Chung, I., and Zhao, X. (2015). DNA break-induced sumoylation is enabled by collaboration between a SUMO ligase and the ssDNA-binding complex RPA. Genes Dev. *29*, 1593–1598.

Churikov, D., Corda, Y., Luciano, P., and Géli, V. (2013). Cdc13 at a crossroads of telomerase action. Front. Oncol. *3*, 39.

Churikov, D., Charifi, F., Simon, M.N., and Géli, V. (2014). Rad59-facilitated acquisition of Y′ elements by short telomeres delays the onset of senescence. PLoS Genet. *10*, e1004736.

Cremona, C.A., Sarangi, P., Yang, Y., Hang, L.E., Rahman, S., and Zhao, X. (2012). Extensive DNA damage-induced sumoylation contributes to replication and repair and acts in addition to the mec1 checkpoint. Mol. Cell *45*, 422–432.

Eckert-Boulet, N., Rothstein, R., and Lisby, M. (2011). Cell biology of homologous recombination in yeast. Methods Mol. Biol. *745*, 523–536.

Galanty, Y., Belotserkovskaya, R., Coates, J., and Jackson, S.P. (2012). RNF4, a SUMO-targeted ubiquitin E3 ligase, promotes DNA double-strand break repair. Genes Dev. *26*, 1179–1195.

Géli, V., and Lisby, M. (2015). Recombinational DNA repair is regulated by compartmentalization of DNA lesions at the nuclear pore complex. BioEssays *37*, 1287–1292.

Geoffroy, M.C., and Hay, R.T. (2009). An additional role for SUMO in ubiquitin-mediated proteolysis. Nat. Rev. Mol. Cell Biol. *10*, 564–568.

Grandin, N., and Charbonneau, M. (2007). Control of the yeast telomeric senescence survival pathways of recombination by the Mec1 and Mec3 DNA damage sensors and RPA. Nucleic Acids Res. *35*, 822–838.

Hector, R.E., Ray, A., Chen, B.-R., Shtofman, R., Berkner, K.L., and Runge, K.W. (2012). Mec1p associates with functionally compromised telomeres. Chromosoma *121*, 277–290.

Horigome, C., Oma, Y., Konishi, T., Schmid, R., Marcomini, I., Hauer, M.H., Dion, V., Harata, M., and Gasser, S.M. (2014). SWR1 and INO80 chromatin remodelers contribute to DNA double-strand break perinuclear anchorage site choice. Mol. Cell *55*, 626–639.

Jackson, S.P., and Durocher, D. (2013). Regulation of DNA damage responses by ubiquitin and SUMO. Mol. Cell *49*, 795–807.

Johnson, F.B., Marciniak, R.A., McVey, M., Stewart, S.A., Hahn, W.C., and Guarente, L. (2001). The Saccharomyces cerevisiae WRN homolog Sgs1p participates in telomere maintenance in cells lacking telomerase. EMBO J. *20*, 905–913.

Kalocsay, M., Hiller, N.J., and Jentsch, S. (2009). Chromosome-wide Rad51 spreading and SUMO-H2A.Z-dependent chromosome fixation in response to a persistent DNA double-strand break. Mol. Cell *33*, 335–343.

Khadaroo, B., Teixeira, M.T., Luciano, P., Eckert-Boulet, N., Germann, S.M., Simon, M.N., Gallina, I., Abdallah, P., Gilson, E., Géli, V., and Lisby, M. (2009). The DNA damage response at eroded telomeres and tethering to the nuclear pore complex. Nat. Cell Biol. *11*, 980–987.

Krogan, N.J., Cagney, G., Yu, H., Zhong, G., Guo, X., Ignatchenko, A., Li, J., Pu, S., Datta, N., Tikuisis, A.P., et al. (2006). Global landscape of protein complexes in the yeast Saccharomyces cerevisiae. Nature *440*, 637–643.

Le, S., Moore, J.K., Haber, J.E., and Greider, C.W. (1999). *RAD50* and *RAD51* define two pathways that collaborate to maintain telomeres in the absence of telomerase. Genetics *152*, 143–152.

Li, S.J., and Hochstrasser, M. (2003). The Ulp1 SUMO isopeptidase: distinct domains required for viability, nuclear envelope localization, and substrate specificity. J. Cell Biol. *160*, 1069–1081.

Loeillet, S., Palancade, B., Cartron, M., Thierry, A., Richard, G.F., Dujon, B., Doye, V., and Nicolas, A. (2005). Genetic network interactions among replication, repair and nuclear pore deficiencies in yeast. DNA Repair (Amst.) *4*, 459–468.

Lydeard, J.R., Jain, S., Yamaguchi, M., and Haber, J.E. (2007). Break-induced replication and telomerase-independent telomere maintenance require Pol32. Nature *448*, 820–823.

McEachern, M.J., and Haber, J.E. (2006). Break-induced replication and recombinational telomere elongation in yeast. Annu. Rev. Biochem. *75*, 111–135.

Mullen, J.R., and Brill, S.J. (2008). Activation of the Slx5-Slx8 ubiquitin ligase by poly-SUMO conjugates. J. Biol. Chem. *283*, 19912–19921.

Nagai, S., Dubrana, K., Tsai-Pflugfelder, M., Davidson, M.B., Roberts, T.M., Brown, G.W., Varela, E., Hediger, F., Gasser, S.M., and Krogan, N.J. (2008). Functional targeting of DNA damage to a nuclear pore-associated SUMO-dependent ubiquitin ligase. Science *322*, 597–602.

Niepel, M., Molloy, K.R., Williams, R., Farr, J.C., Meinema, A.C., Vecchietti, N., Cristea, I.M., Chait, B.T., Rout, M.P., and Strambio-De-Castillia, C. (2013). The nuclear basket proteins Mlp1p and Mlp2p are part of a dynamic interactome including Esc1p and the proteasome. Mol. Biol. Cell *24*, 3920–3938.

Oza, P., Jaspersen, S.L., Miele, A., Dekker, J., and Peterson, C.L. (2009). Mechanisms that regulate localization of a DNA double-strand break to the nuclear periphery. Genes Dev. *23*, 912–927.

Palancade, B., Liu, X., Garcia-Rubio, M., Aguilera, A., Zhao, X., and Doye, V. (2007). Nucleoporins prevent DNA damage accumulation by modulating Ulp1-dependent sumoylation processes. Mol. Biol. Cell *18*, 2912–2923.

Pfeiffer, V., and Lingner, J. (2013). Replication of telomeres and the regulation of telomerase. Cold Spring Harb. Perspect. Biol. *5*, a010405–a010405.

Potts, P.R., and Yu, H. (2007). The SMC5/6 complex maintains telomere length in ALT cancer cells through SUMOylation of telomere-binding proteins. Nat. Struct. Mol. Biol. *14*, 581–590.

Psakhye, I., and Jentsch, S. (2012). Protein group modification and synergy in the SUMO pathway as exemplified in DNA repair. Cell *151*, 807–820.

Reindle, A., Belichenko, I., Bylebyl, G.R., Chen, X.L., Gandhi, N., and Johnson, E.S. (2006). Multiple domains in Siz SUMO ligases contribute to substrate selectivity. J. Cell Sci. *119*, 4749–4757.

Sacher, M., Pfander, B., Hoege, C., and Jentsch, S. (2006). Control of Rad52 recombination activity by double-strand break-induced SUMO modification. Nat. Cell Biol. *8*, 1284–1290.

Sarangi, P., and Zhao, X. (2015). SUMO-mediated regulation of DNA damage repair and responses. Trends Biochem. Sci. *40*, 233–242.

Schober, H., Ferreira, H., Kalck, V., Gehlen, L.R., and Gasser, S.M. (2009). Yeast telomerase and the SUN domain protein Mps3 anchor telomeres and repress subtelomeric recombination. Genes Dev. *23*, 928–938.

Su, X.A., Dion, V., Gasser, S.M., and Freudenreich, C.H. (2015). Regulation of recombination at yeast nuclear pores controls repair and triplet repeat stability. Genes Dev. *29*, 1006–1017.

Taddei, A., and Gasser, S.M. (2012). Structure and function in the budding yeast nucleus. Genetics *192*, 107–129.

Taddei, A., Hediger, F., Neumann, F.R., Bauer, C., and Gasser, S.M. (2004). Separation of silencing from perinuclear anchoring functions in yeast Ku80, Sir4 and Esc1 proteins. EMBO J. *23*, 1301–1312.

Tan, W., Wang, Z., and Prelich, C. (2013). Physical and genetic interactions between Uls1 and the Slx5-Slx8 SUMO-targeted ubiquitin ligase. G3 (Bethesda, Md) *3*, 771–780.

Teng, S.C., and Zakian, V.A. (1999). Telomere-telomere recombination is an efficient bypass pathway for telomere maintenance in Saccharomyces cerevisiae. Mol. Cell. Biol. *19*, 8083–8093.

Teng, S.C., Chang, J., McCowan, B., and Zakian, V.A. (2000). Telomerase-independent lengthening of yeast telomeres occurs by an abrupt Rad50p-dependent, Rif-inhibited recombinational process. Mol. Cell *6*, 947–952.

Texari, L., Dieppois, G., Vinciguerra, P., Contreras, M.P., Groner, A., Letourneau, A., and Stutz, F. (2013). The nuclear pore regulates GAL1 gene transcription by controlling the localization of the SUMO protease Ulp1. Mol. Cell *51*, 807–818.

Therizols, P., Fairhead, C., Cabal, G.G., Genovesio, A., Olivo-Marin, J.C., Dujon, B., and Fabre, E. (2006). Telomere tethering at the nuclear periphery is essential for efficient DNA double strand break repair in subtelomeric region. J. Cell Biol. *172*, 189–199.

Wellinger, R.J., and Zakian, V.A. (2012). Everything you ever wanted to know about *Saccharomyces cerevisiae* telomeres: beginning to end. Genetics *191*, 1073–1105.

Xie, Y., Kerscher, O., Kroetz, M.B., McConchie, H.F., Sung, P., and Hochstrasser, M. (2007). The yeast Hex3.Slx8 heterodimer is a ubiquitin ligase stimulated by substrate sumoylation. J. Biol. Chem. *282*, 34176–34184.

Zhao, X., Wu, C.Y., and Blobel, G. (2004). Mlp-dependent anchorage and stabilization of a desumoylating enzyme is required to prevent clonal lethality. J. Cell Biol. *167*, 605–611.